frontiers in Pharmacology

ORIGINAL RESEARCH
published: 01 March 2016
doi: 10.3389/fphar.2016.00039

Effects of Amiodarone and *N*-desethylamiodarone on Cardiac Voltage-Gated Sodium Channels

*Mohammad-Reza Ghovanloo, Mena Abdelsayed and Peter C. Ruben**

Department of Biomedical Physiology and Kinesiology, Simon Fraser University, Burnaby, BC, Canada

Amiodarone (AMD) is a potent antiarrhythmic drug with high efficacy for treating atrial fibrillation and tachycardia. The pharmacologic profile of AMD is complex. AMD possesses biophysical characteristics of all of class I, II, III, and IV agents. Despite its adverse side effects, AMD remains the most commonly prescribed antiarrhythmic drug. AMD was described to prolong the QT interval and can lead to torsades de pointes. Our goal was to study the effects of AMD on peak and late sodium currents ($I_{Na,P}$ and $I_{Na,L}$) and determine whether these effects change as AMD is metabolized into *N*-desethylamiodarone (DES). We hypothesized that AMD and DES block both $I_{Na,P}$ and $I_{Na,L}$ with similar profiles due to structural similarities. Given the inherent small amounts of $I_{Na,L}$ in $Na_V1.5$, we screened AMD and DES against the Long QT-3-causing mutation, ΔKPQ, to better detect any drug-mediated effect on $I_{Na,L}$. Our results show that AMD and DES do not affect WT or ΔKPQ activation; however, both drugs altered the apparent valence of steady-state fast-inactivation. In addition, AMD and DES preferentially block ΔKPQ peak conductance compared to WT. Both compounds significantly increase $I_{Na,L}$ and window currents. We conclude that both compounds have pro-arrhythmic effects on $Na_V1.5$, especially ΔKPQ; however, DES seems to have a greater pro-arrhythmic effect than AMD.

Keywords: amiodarone, *N*-desethylamiodarone, electrophysiology, long QT, Nav1.5

OPEN ACCESS

Edited by:
Aida Salameh,
Heart Centre University of Leipzig, Germany

Reviewed by:
Carmen Valenzuela,
Instituto de Investigaciones Biomédicas CSIC-UAM, Spain
Stefan Dhein,
University of Leipzig, Germany
Torsten Christ,
University Medical Center Eppendorf, Germany

****Correspondence:***
Peter C. Ruben
pruben@sfu.ca

Specialty section:
This article was submitted to Cardiovascular and Smooth Muscle Pharmacology, a section of the journal Frontiers in Pharmacology

Received: *12 December 2015*
Accepted: *12 February 2016*
Published: *01 March 2016*

Citation:
Ghovanloo M-R, Abdelsayed M and Ruben PC (2016) Effects of Amiodarone and N-desethylamiodarone on Cardiac Voltage-Gated Sodium Channels. Front. Pharmacol. 7:39. doi: 10.3389/fphar.2016.00039

INTRODUCTION

In the 1960s, an iodine-containing benzofuran compound called amiodarone (AMD) was developed as a therapeutic vasodilator (Phillips and Bauman, 1995). Decades of research and clinical trials have shown the effects of AMD in a range of organ systems. AMD slowly became a widely used antiarrhythmic drug, with a high efficacy for treating conditions including atrial fibrillation and tachycardia (Pollak, 1998). The pharmacologic profile of this drug is complex. Although AMD has been classified primarily as a class III antiarrhythmic drug, it also has biophysical characteristics of class I, II, and IV agents in that it blocks L-type calcium, potassium, and sodium currents (Singh and Vaughan Williams, 1970; Kodama et al., 1997; Nattel and Singh, 1999; Wu et al., 2008). AMD is the most commonly prescribed antiarrhythmic drug despite its potentially serious side effects, including adverse effects on thyroid glands, the pulmonary system, and the liver (Danzi and Klein, 2015).

In experimental cardiac preparations, the use of AMD is associated with prolongation of the QT interval and action potential duration (APD). These events may lead to torsades de pointes (Tarapues et al., 2014). AMD has a higher selectivity for the potassium and sodium channels that

are expressed in atrial as opposed to ventricular myocytes (Suzuki et al., 2013). The atrial selectivity of sodium channel block may contribute to the treatment of atrial fibrillation (Antzelevitch and Burashnikov, 2009; Burashnikov and Antzelevitch, 2013). However, AMD's potency to prolong the QT interval has led to its prohibition in patients with Long-QT Syndrome (Digby et al., 2011; Franz et al., 2014).

Long-term treatments with AMD is suggested to induce remodeling of ion-channel expression in a dose-dependent manner, leading to electrophysiological variations. Therefore, in addition to directly affecting membrane proteins, AMD also modifies the levels of ion-channel transcripts (Le Bouter et al., 2004).

Although several Cytochrome P450 (CYP) subtypes may contribute to metabolism of any given compound, the primary enzymes involved in the AMD metabolism are CYP3A4 and CYP2C8 (Ohyama et al., 2000; Zahno et al., 2011). AMD has a relatively long half-life of 40–50 days (Zipes et al., 1984). The full metabolism of AMD gives rise to 22 phase I and 11 phase II products (Deng et al., 2011). AMD's most prominent metabolite is produced as a result of a *N*-deethylation reaction catalyzed by CYP3A4, producing DES, which is a pharmacologically active compound (Deng et al., 2011).

In a classic study conducted by Pallandi and Campbell (1987) on guinea-pig ventricular myocardium, it was determined that at clinically relevant levels, AMD and DES exhibit both class I and class III effects. The class I effects (on sodium channels) are rate dependent, which in conjunction with the class III effects (on potassium channels) may increase APD and reduce V_{max} (Pallandi and Campbell, 1987).

Despite the potency of AMD as an antiarrhythmic agent and the already existing body of knowledge, its effects on sodium channels are still poorly understood. We sought to study the effects of AMD on peak and late sodium currents ($I_{Na,P}$ and $I_{Na,L}$), and determine whether these effects change as AMD metabolizes into DES. We hypothesized that both AMD and DES block $I_{Na,P}$ and $I_{Na,L}$ with similar profiles due to their structural similarities. Given the low amplitude of $I_{Na,L}$ in $Na_V1.5$, we used the LQT-3 mutation, ΔKPQ, to increase $I_{Na,L}$ and thus better detect potential drug-mediated effect on $I_{Na,L}$. The mutant phenotype associated with ΔKPQ is manifested in the presence of large $I_{Na,L}$ due to the deletion of three amino acids (Lysine, Proline, Glutamine) in the linker region between domains III and IV in $Na_V1.5$ (Wang et al., 1995). This is a hot-spot region in $Na_V1.5$ since it elicits fast-inactivation (Chandra et al., 1998). We report that AMD and DES have similar effects on the voltage-dependence of fast-inactivation and the amplitude of $I_{Na,L}$, and can therefore contribute to pro-arrhythmic effects.

MATERIALS AND METHODS

Cell Culture

Chinese hamster ovary (CHO) cells were transiently transfected with cDNA encoding either wild-type or the ΔKPQ mutant form

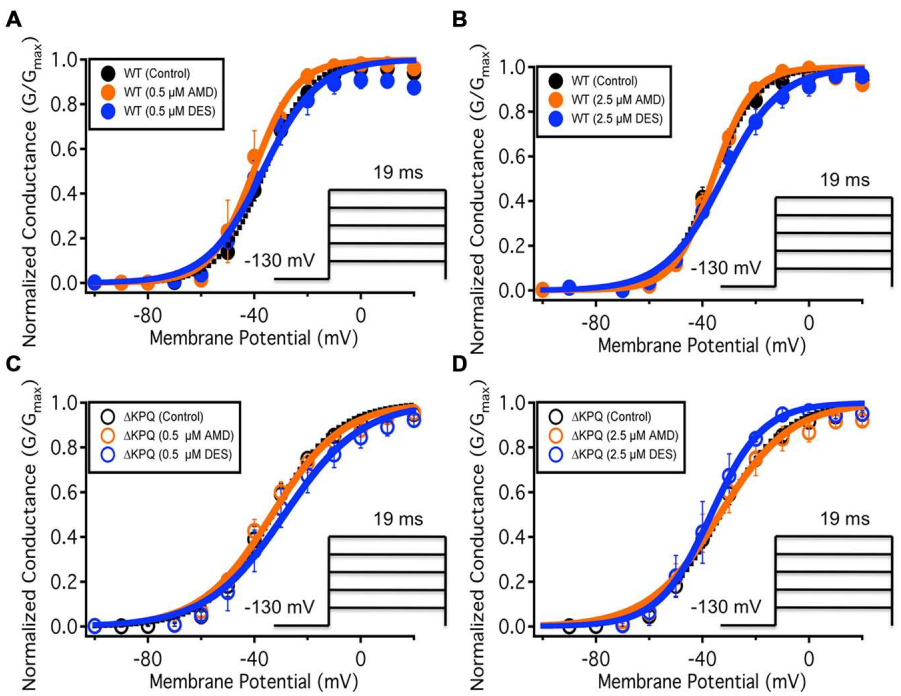

FIGURE 1 | (A–D) Show the voltage dependence of activation as normalized conductance plotted against membrane potential. The black curves represent the WT $Na_V1.5$ or ΔKPQ conductance with no drug perfusion, the orange curves represent $Na_V1.5$ or ΔKPQ conductance after either 0.5 or 2.5 μM AMD perfusion, and the blue curves represent $Na_V1.5$ or ΔKPQ conductance after either 0.5 or 2.5 μM DES perfusion.

of $Na_V1.5$. Transfection was done according to the PolyFect transfection protocol. After each set of transfections, a minimum of 8 h incubation was allowed before platting. Dr. Robert Kass generously provided *SCN5A* cDNA encoding the ΔKPQ mutation.

Electrophysiology

Whole-cell patch clamp recordings were performed in an extracellular solution containing (in mM): 140 NaCl, 4 KCl, 2 $CaCl_2$, 1 $MgCl_2$, 10 HEPES. Solutions were adjusted to pH 7.4 with CsOH. Pipettes were filled with intracellular solution, containing (in mM): 120 CsF, 20 CsCl, 10 NaCl, 10 HEPES, pH 7.4. All recordings were made using an EPC-9 patch-clamp amplifier (HEKA Elektronik, Lambrecht, Germany) digitized at 20 kHz via an ITC-16 interface (Instrutech, Great Neck, NY, USA). Voltage clamping and data acquisition were controlled using PatchMaster/FitMaster software (HEKA Elektronik, Lambrecht, Germany) running on an Apple iMac. Current was low-pass-filtered at 5 kHz. Leak subtraction was performed automatically by software using a P/4 procedure following the test pulse. Gigaohm seals were allowed to stabilize in the on-cell configuration for 1 min prior to establishing the whole-cell configuration. Series resistance was less than 5 MΩ for all recordings. Series resistance compensation up to 80% was used when necessary. All data were acquired at least 5 min after attaining the whole-cell configuration, and cells were allowed to incubate 5 min after drug application prior to data collection. Before each protocol, the membrane potential was hyperpolarized to −130 mV to insure complete removal of both fast-inactivation and slow-inactivation. Leakage and capacitive currents were subtracted with a P/4 protocol. All experiments were conducted at room temperature at 22°C.

Analysis

Analysis and graphing were done using FitMaster software (HEKA Elektronik) and Igor Pro (Wavemetrics, LakeOswego, OR, USA) with statistical information derived using JMP statistical software version 11. All data acquisition and analysis programs were run on an Apple iMac (Apple Computer). A two-way analysis of variance (ANOVA) was used to compare the means responses [activation, peak current block, steady-state fast-inactivation (SSFI), late currents, and window currents] between channel variant, and compound. Channel variant, compound and the way interaction involving the two were considered to be fixed effects in the model. Channel variant had two levels (WT, ΔKPQ) and compound had six levels (0, 0.5, and 2.5 μM AMD and DES). *Post hoc* tests using the Tukey Kramer adjustment were used to compare mean responses between pairs of channel variant and/or compounds. A level of significance $\alpha = 0.05$ was used in all overall *post hoc* tests, and effects with *p*-values less then 0.05 were considered to be statistically

TABLE 1 | Steady-state activation.

	GV – $V_{1/2}$ (mV)	GV – z (slope)	*n*
Wild-type			
$Na_V1.5$			
Control	−35.5 ± 1.63	3.79 ± 0.29	20
AMD 0.5 μM	−45.7 ± 4.42	3.91 ± 0.69	4
AMD 2.5 μM	−36.1 ± 1.45	3.54 ± 0.15	4
DES 0.5 μM	−35.5 ± 3.57	3.25 ± 0.54	7
DES 2.5 μM	−32.4 ± 1.87	2.67 ± 0.40	5
ΔKPQ			
$Na_V1.5$			
Control	−33.6 ± 2.35	3.25 ± 0.34	20
AMD 0.5 μM	−34.8 ± 2.75	2.29 ± 0.24	5
AMD 2.5 μM	−35.1 ± 4.61	2.63 ± 0.26	6
DES 0.5 μM	−31.1 ± 5.34	2.26 ± 0.16	4
DES 2.5 μM	−31.1 ± 3.10	2.66 ± 0.53	4

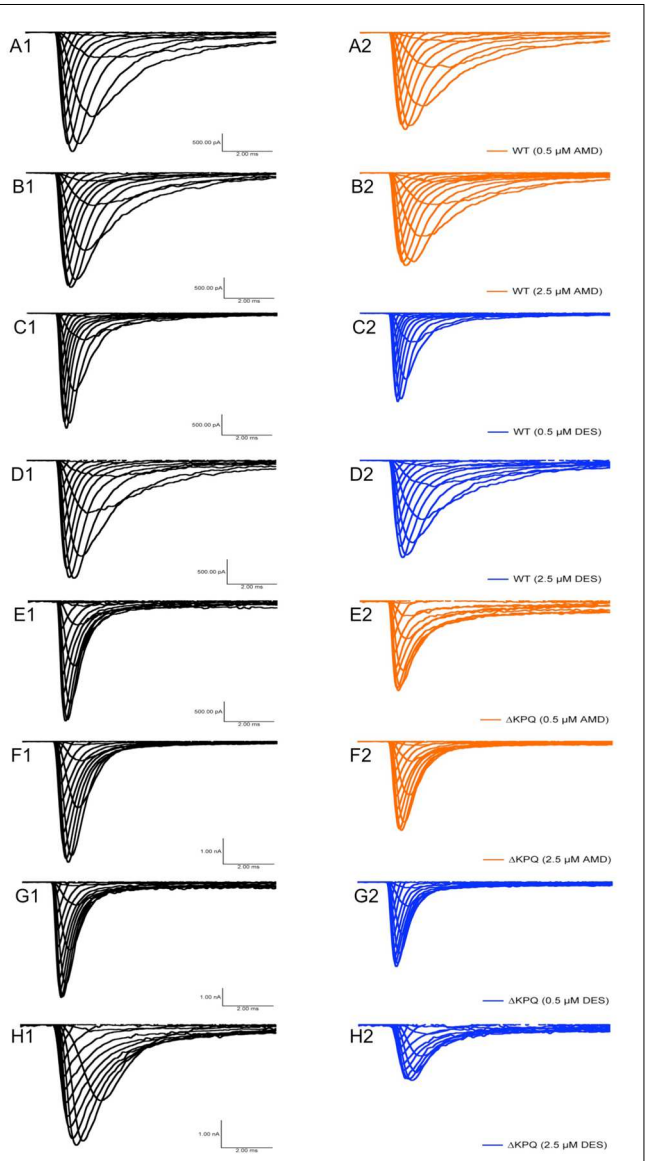

FIGURE 2 | Current amplitude plotted versus time duration. The traces show the variation in current levels before and after AMD and DES perfusion.

significant. All values reported are given as mean ± standard error of means for *n* cells.

Activation Protocols

To determine the voltage dependence of activation, we measured the peak current amplitude at test pulse potentials ranging from −100 to +80 mV in increments of +10 mV for 20 ms. Channel conductance (G) was calculated from peak I_{Na}:

$$G_{Na} = I_{Na}/V - E_{Na}$$

where G_{Na} is conductance, I_{Na} is peak sodium current in response to the command potential V, and E_{Na} is the Nernst equilibrium potential. Calculated values for conductance were fit with the Boltzmann equation:

$$G/G_{max} = 1/(1 + \exp[-ze_0[V_m - V_{1/2}]/kT])$$

where G/G_{max} is normalized conductance amplitude, V_m is the command potential, z is the apparent valence, e_0 is the elementary charge, $V_{1/2}$ is the midpoint voltage, k is the Boltzmann constant, and T is temperature in °K.

Steady-State Fast-Inactivation Protocols

The voltage-dependence of fast-inactivation was measured by preconditioning the channels to a hyperpolarizing potential of −130 mV and then eliciting pre-pulse potentials that ranged from −170 to +10 mV in increments of 10 mV for 500 ms, followed by a 10 ms test pulse during which the voltage was stepped to 0 mV. Normalized current amplitude as a function of voltage was fit using the Boltzmann equation:

$$I/I_{max} = 1/(1 + \exp(-ze_0(V_M - V_{1/2})/kT)$$

where I_{max} is the maximum test pulse current amplitude.

TABLE 2 | Peak I_{Na} block.

	Peak I_{Na} block	*n*
Wild-type		
zNa_V1.5		
AMD 0.5 μM	0.05 ± 0.11	3
AMD 2.5 μM	0.14 ± 0.12	6
DES 0.5 μM	0.32 ± 0.05	7
DES 2.5 μM	0.12 ± 0.13	6
ΔKPQ		
Na_V1.5		
AMD 0.5 μM	0.39 ± 0.12	6
AMD 2.5 μM	0.38 ± 0.28	4
DES 0.5 μM	0.28 ± 0.04	4
DES 2.5 μM	0.55 ± 0.12	6

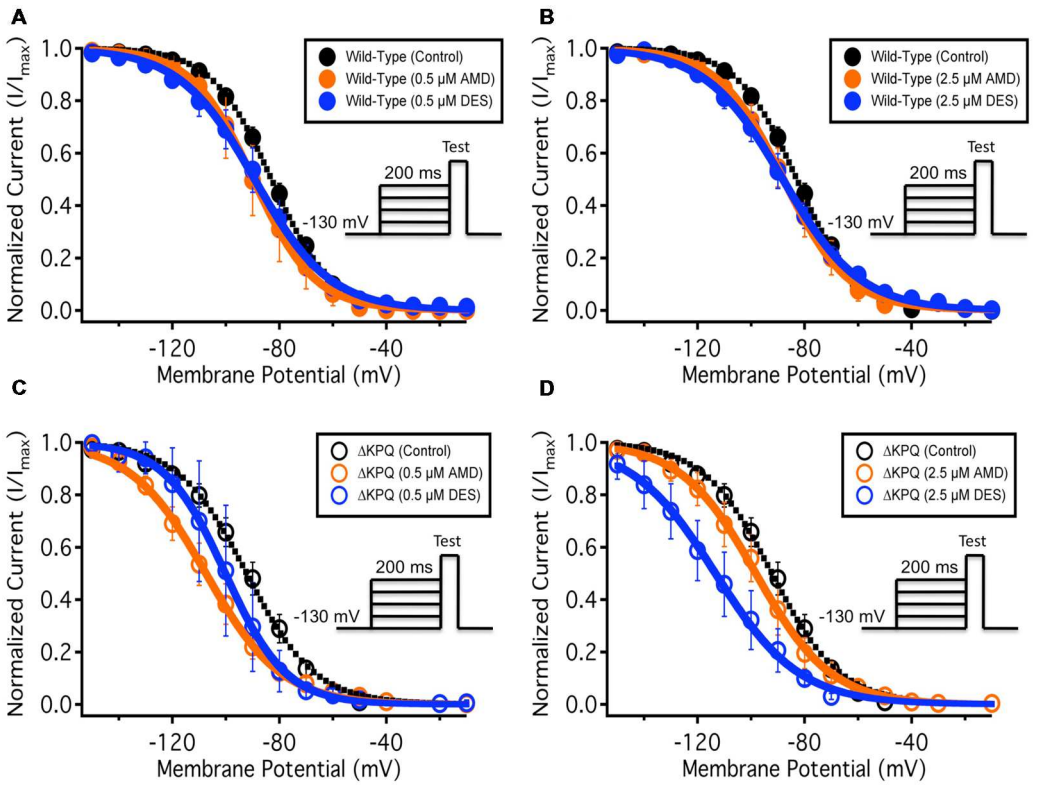

FIGURE 3 | (A–D) Show the voltage dependence of steady-state fast-inactivation as normalized current plotted against membrane potential. The black curves represent the WT $Na_v1.5$ or ΔKPQ SSFI with no drug perfusion, the orange curves represent $Na_v1.5$ or ΔKPQ SSFI after either 0.5 or 2.5 μM AMD perfusion, and the blue curves represent $Na_v1.5$ or ΔKPQ SSFI after either 0.5 or 2.5 μM DES perfusion.

Window Current Measurements

Window currents were measured by maintaining the voltage at −130 mV for 1 s. Then, the voltage was ramped to 20 mV for 20 ms, at a rate of 0.3 mV/ms. The channels were then recovered from inactivation at the voltage of −130 mV for 20 ms.

Drug Preparation

We sought to study the effects of AMD and DES on cardiac voltage-gated sodium channels using their therapeutic serum concentrations which, for both compounds, is 2.5 μM (Sheldon et al., 1989). However, xenobiotic concentrations decrease over time; therefore, to assess the effects of these reductions, our experiments were also conducted at 0.5 μM AMD and DES. To ensure no run-down of sodium currents is taking place, electrophysiological recordings were taken on average 3–5 min after AMD or DES perfusion, until current levels were stabilized.

Simulations

Action potentials were simulated in OpenCell (Physiome Project) with the 2004 Hund-Rudy Canine ventricular cell model (Rate Dependence and Regulation of Action Potential and Calcium Transient in a Canine Cardiac Ventricular Cell Model, Hund and Rudy, 2004. http://models.cellml.org/exposure/f4b7120aa512c7f5e7a0664abcee3e8b/hund_rudy_2004_b.cellml/view 6.33 pm 12th January 2016 CellML author(s): Catherine Lloyd) (Hund and Rudy, 2004; Lloyd et al., 2008).

RESULTS

Activation

We examined the effects of AMD and DES on activation in $Na_V1.5$ and ΔKPQ channels. **Figure 1** shows normalized conductance plotted as a function of membrane potential under control solutions (black curves with filled circles), in AMD solutions (orange curves with filled circles), and DES solutions (blue curves with filled circles) in WT and ΔKPQ $Na_V1.5$ channels. AMD and DES cause no significant effects on the voltage dependence of activation. There were no significant shifts in the midpoint or apparent valence at either 0.5 or 2.5 μM of AMD or DES in either $Na_V1.5$ or ΔKPQ ($p > 0.05$; **Table 1**). Current traces from the eight experimental conditions (before and after AMD or DES perfusion) are shown in (**Figure 2**).

TABLE 3 | Steady-state fast-inactivation.

	SSFI – $V_{1/2}$ (mV)	SSFI – z (slope)	*n*
Wild-type			
$Na_V1.5$			
Control	−83.0 ± 1.82	−2.68 ± 0.10	20
AMD 0.5 μM	−89.1 ± 6.04	−2.81 ± 0.33	4
AMD 2.5 μM	−87.4 ± 3.79	−2.36 ± 0.15	7
DES 0.5 μM	−89.5 ± 4.38	−2.19 ± 0.12	7
DES 2.5 μM	−88.4 ± 3.00	−1.89 ± 0.14	5
ΔKPQ			
$Na_V1.5$			
Control	−92.3 ± 3.06	−2.79 ± 0.15	20
AMD 0.5 μM	−107.3 ± 3.69	−2.08 ± 0.16	6
AMD 2.5 μM	−94.9 ± 5.21	−2.22 ± 0.19	5
DES 0.5 μM	−100.3 ± 4.86	−2.74 ± 0.34	4
DES 2.5 μM	−107.8 ± 5.24	−2.38 ± 0.21	5

Peak Current Block

Amiodarone is a sodium channel blocker. To determine whether there is a difference between AMD and DES in their ability to block INa, we compared the peak current in each channel variant before and after the perfusion of either compound at one of the noted concentrations. Although current block was seen across all conditions, there was a significant mutant effect, indicating that both the mother compound, AMD, and its metabolite, DES, block

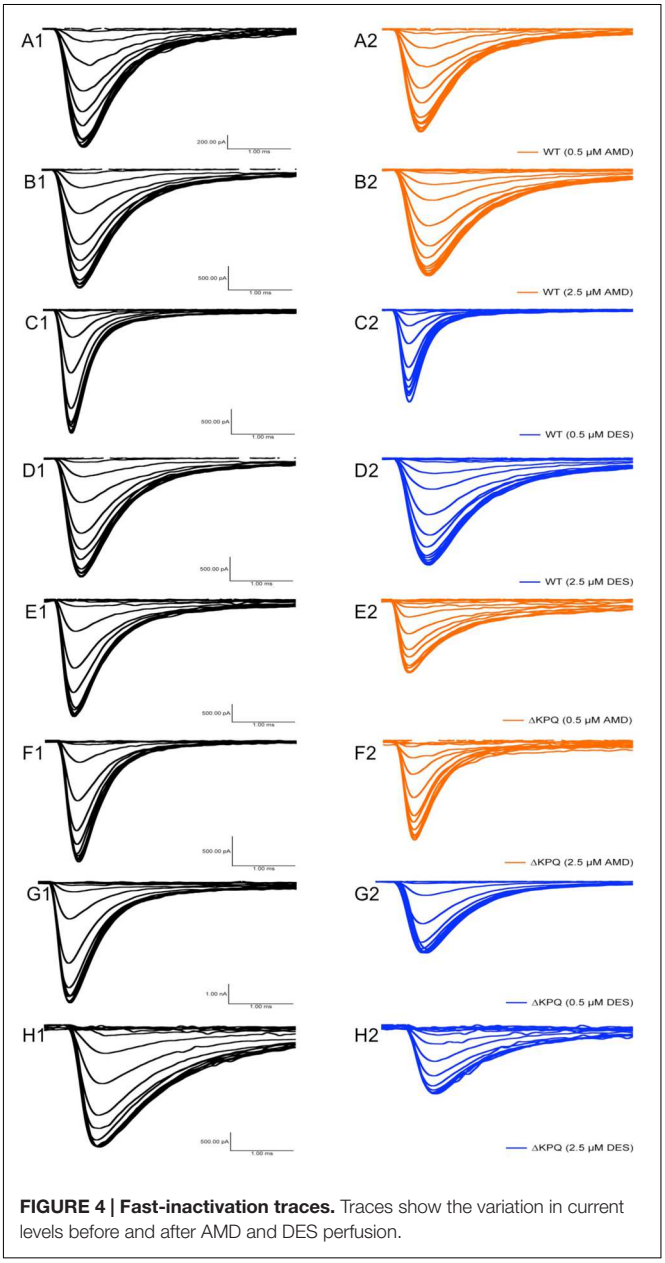

FIGURE 4 | Fast-inactivation traces. Traces show the variation in current levels before and after AMD and DES perfusion.

ΔKPQ more than they block $Na_V1.5$ ($p < 0.05$; **Table 2**). The largest block was observed in ΔKPQ mutants at 2.5 μM DES (**Table 2**).

Steady-State Fast-Inactivation

To quantify the effects of each compound at 0.5 and 2.5 μM on fast-inactivation, we compared the apparent valence (z) and midpoint ($V_{1/2}$) from Boltzmann fits to SSFI data for $Na_V1.5$ (**Figures 3A,B**) and ΔKPQ (**Figures 3C,D**). Normalized current amplitudes were plotted as a function of pre-pulse potential (**Figure 3**). The apparent valence of SSFI of ΔKPQ (2.79 ± 0.15) was greater than that of WT $Na_V1.5$ (2.68 ± 0.10). AMD and DES at 0.5 and 2.5 μM significantly reduced the apparent valence of SSFI in both $Na_V1.5$ and ΔKPQ ($p < 0.05$; **Table 3**). The $V_{1/2}$ of ΔKPQ was significantly hyperpolarized compared to WT ($p < 0.05$); however, there were no significant shifts in the $V_{1/2}$ of either channel variant with AMD or DES at either concentration ($p > 0.05$; **Table 3**). Representative traces are shown in (**Figure 4**).

Late Sodium Currents

The presence of $I_{Na,L}$ is an indicator of destabilized fast-inactivation. We show representative normalized current traces of $I_{Na,L}$ for the two channel variants across all conditions (**Figure 5**). Although, both compounds appear to have statistically significant effects on elevating $I_{Na,L}$ levels ($p < 0.01$), the most prominent $I_{Na,L}$ increase was seen upon the perfusion of 2.5 μM DES on ΔKPQ (**Figure 6A**; **Table 4**). Therefore, therapeutic levels of DES potently further destabilize fast-inactivation in ΔKPQ mutants.

Sodium Window Currents

Changes in both steady-state activation and fast-inactivation can lead to differences in the window current. Representative normalized traces of sodium window currents from all conditions are shown in (**Figure 7**). Similar to $I_{Na,L}$, there was an significant compound effect on the sodium window currents ($p < 0.05$), where the greatest effect was seen in ΔKPQ at 2.5 μM DES (**Figure 6B**; **Table 5**).

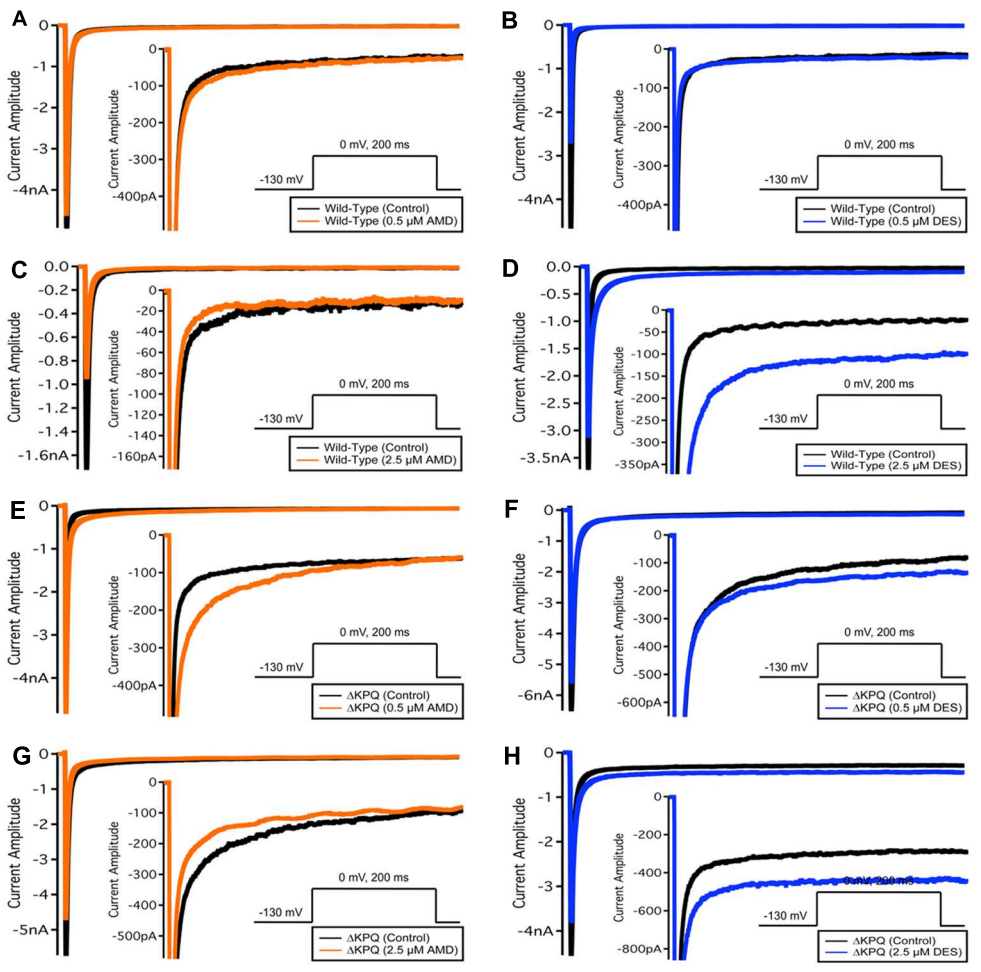

FIGURE 5 | Representative normalized current traces of INa_L. (A–H) Each panel shows the INa_L in $Na_V1.5$ or ΔKPQ before and after the perfusion of either 0.5 or 2.5 μM AMD or DES. Black curves represent control (0 μM drug solution), orange curves represent AMD at either 0.5 or 2.5 μM, and blue curves represent DES at either 0.5 or 2.5 μM.

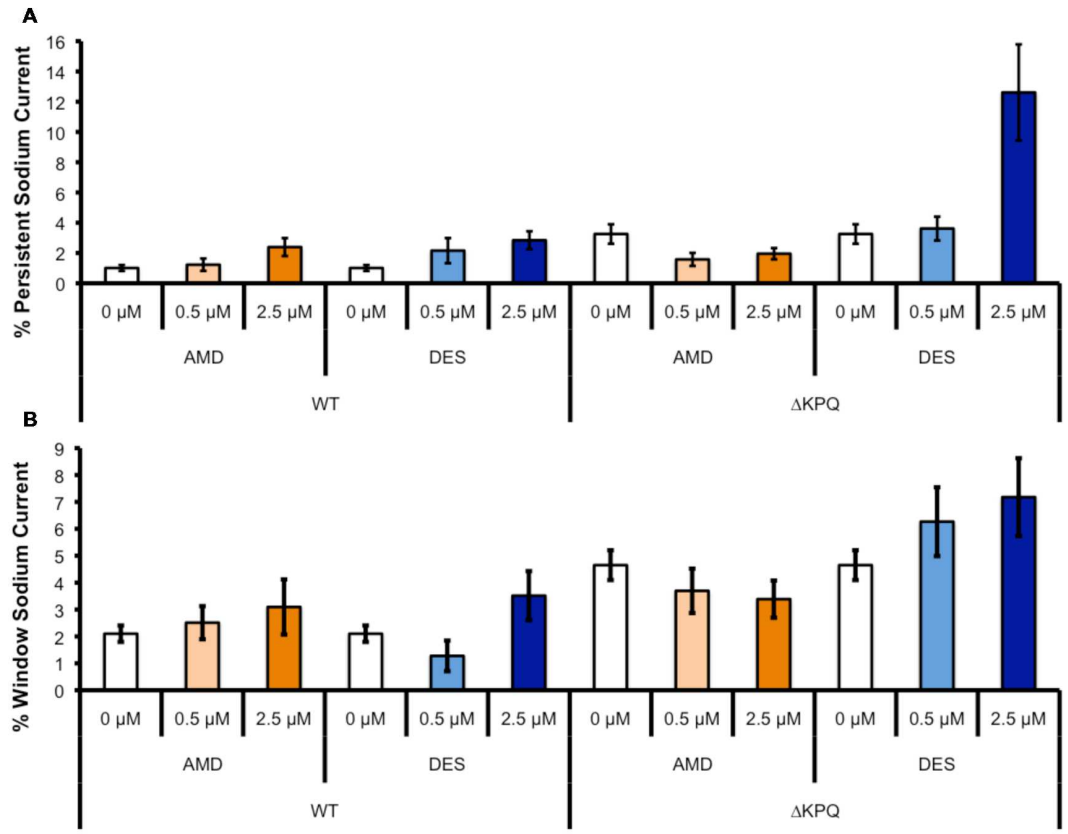

FIGURE 6 | (A) Shows the percentage of persistent sodium currents in either WT $Na_V1.5$ or ΔKPQ channels after the perfusion of 0, 0.5, or 2.5 μM AMD (light or dark orange) or DES (light or dark blue). **(B)** Shows the percentage of window sodium currents in either WT $Na_V1.5$ or ΔKPQ channels after the perfusion of 0, 0.5, or 2.5 μM AMD (light or dark orange) or DES (light or dark blue).

Action Potential Modeling

The duration of action potentials plays a fundamental role in the functioning of cardiac myocytes. The alteration of any contributors in action potential generation and maintenance could lead to detrimental effects such as life-threatening arrhythmias. In order to determine whether the observed compound-mediated fast-inactivation destabilization can lead to pro-arrhythmogenicity, we used the Hund-Rudy Canine model to simulate a cardiac action potential (**Figure 8**). The simulation results indicate that the extent of action potential prolongation is consistent with our experimental data showing compound-mediated exacerbation in $I_{Na,L}$. As expected, the APD of ΔKPQ was longer than $Na_V1.5$, hence the LQT phenotype. Furthermore, the model suggests that the biggest pro-arrhythmogenic effect occurs at 2.5 μM DES in ΔKPQ mutants (**Figure 8**; **Table 6**).

TABLE 4 | Persistent I_{Na}.

	Persistent I_{Na}	*n*
Wild-type		
$Na_V1.5$		
Control	0.88 ± 0.16	23
AMD 0.5 μM	1.23 ± 0.41	6
AMD 2.5 μM	2.39 ± 0.59	6
DES 0.5 μM	2.16 ± 0.83	6
DES 2.5 μM	2.84 ± 0.59	5
ΔKPQ		
$Na_V1.5$		
Control	2.79 ± 0.55	18
AMD 0.5 μM	2.89 ± 1.35	6
AMD 2.5 μM	2.62 ± 0.73	6
DES 0.5 μM	3.62 ± 0.79	5
DES 2.5 μM	12.6 ± 3.18	4

DISCUSSION

Since its development, the use of AMD as a therapeutic has fluctuated due to occasional reports of toxicity in some individuals. These safety issues have resulted in AMD being regarded as a dangerous drug; however, the efficacy of this drug against certain conditions, such as atrial fibrillation, is well-established.

We performed the first detailed study on the effects of AMD on cardiac voltage-gated sodium channels. We included DES, a

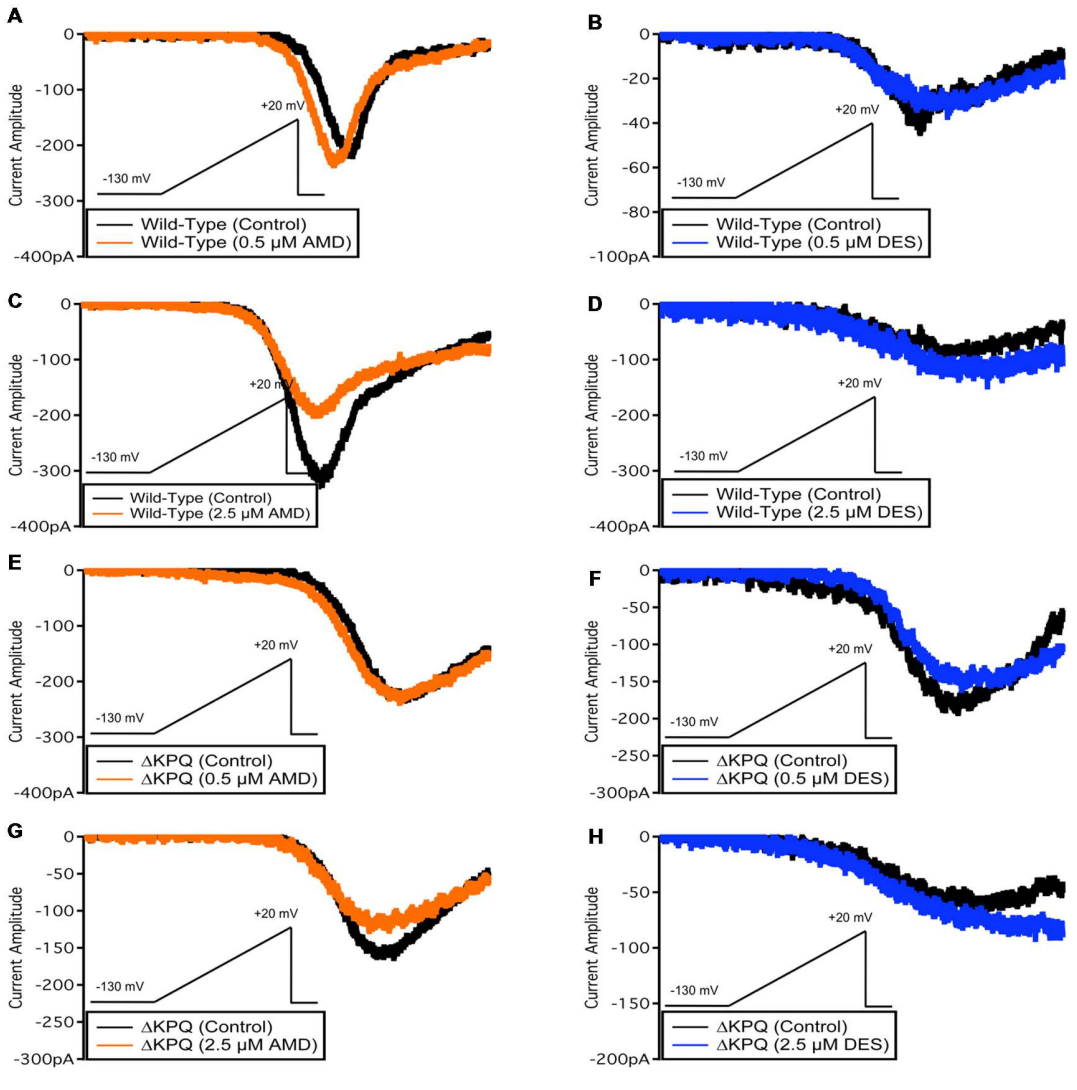

FIGURE 7 | Representative sodium window currents. (A–H) Each panel shows the window currents in $Na_V1.5$ or ΔKPQ before and after the perfusion of either 0.5 or 2.5 μM AMD or DES. Black curves represent control (0 μM drug solution), orange curves represent AMD at either 0.5 or 2.5 μM, and blue curves represent DES at either 0.5 or 2.5 μM.

physiologically active metabolite of AMD, into our study, and compared the effects of AMD and DES on biophysical properties in WT $Na_V1.5$ and ΔKPQ, a channel variant with an exaggerated late current. Neither AMD nor DES affect the voltage dependence of activation or SSFI. However, a decrease in the apparent valence in SSFI of both channels suggests that the compounds reduce the $Na_V1.5$ and ΔKPQ charge sensitivities.

Although AMD has been recognized as a sodium channel blocker, DES has not been fully characterized with respect to its effects on sodium channels. Here, we show that DES also blocks sodium channels. Interestingly, both compounds have a significant preference in blocking ΔKPQ compared to WT $Na_V1.5$.

Our results indicate that DES significantly increases both $I_{Na,L}$ and window currents in ΔKPQ mutants. Given that the presence of $I_{Na,L}$ is a manifestation of the failure to fast-inactivate, we conclude that DES further disrupts ΔKPQ fast-inactivation.

In an earlier study, Maltsev et al. (2001) performed electrophysiological studies on cardiac cells isolated from failing human hearts. They concluded that AMD blocks late sodium currents in these cells. However, within the same study they mentioned that the interpretation of their results is rather complicated due to the $I_{Na,L}$ density variations in the cardiomyocytes from different patients (Maltsev et al., 2001). These variations point to the differences in the genetic background present in isolated myocytes, which may have led to the observed results in that study. In order to reduce the confounding effects of the rather complex genetic background in human myocytes, we performed our studies in the simpler CHO cells. This allowed us to understand the biophysics of

TABLE 5 | Ramp I_{Na}.

	Ramp I_{Na}	*n*
Wild-type		
$Na_V1.5$		
Control	1.77 ± 0.25	19
AMD 0.5 μM	2.51 ± 0.62	5
AMD 2.5 μM	3.10 ± 1.02	4
DES 0.5 μM	1.28 ± 0.57	6
DES 2.5 μM	3.52 ± 0.91	4
ΔKPQ		
$Na_V1.5$		
Control	4.30 ± 0.47	22
AMD 0.5 μM	1.84 ± 0.82	5
AMD 2.5 μM	3.39 ± 0.69	5
DES 0.5 μM	6.27 ± 1.28	6
DES 2.5 μM	7.18 ± 1.45	5

the interactions between AMD/DES and $Na_V1.5$/ΔKPQ on a fundamental level, and then apply that information to a generic myocyte action potential model using computer simulations.

In another study conducted by Wu et al. (2008) attempting to characterize AMD, sea anemone toxin II (ATX-II) was used to induce $I_{Na,L}$ in $Na_V1.5$. This study concluded that ATX-II-mediated $I_{Na,L}$ is blocked by AMD (Wu et al., 2008). These results led us to initially hypothesize that AMD and DES would block both $I_{Na,L}$ and $I_{Na,P}$; however, ATX-II is also a chemical agent that interacts with sodium channels. To eliminate inter-compound interactions between ATX-II and AMD or DES, we used ΔKPQ. The pro-arrhythmic effects of these compounds on $I_{Na,L}$ were, particularly notable. Mutational studies in $Na_V1.2$ indicate that ATX-II tends to interact close to the glutamic acid residue at position 1613 on the DIVS3-S4 extracellular loop (Rogers et al., 1996). Considering AMD and DES were perfused on the extracellular side of the channels in our experiments, along with previous findings in $Na_V1.2$, our contradictory results to Wu et al. (2008) seem justified. We predict that the mode of action of AMD may involve interactions with DIVS3-S4 of the sodium channel. This would indicate that AMD outcompetes ATX-II for binding sites on the sodium channel. This hypothesis may explain the decrease in $I_{Na,L}$ in ATX-II-treated channels; however, this hypothesis needs to be tested in future studies.

It is well-known that the prolongation of the QT interval on the electrocardiogram is a prominent risk factor for arrhythmias, which may lead to sudden death. There are many pathophysiological mechanisms that may underlie this prolongation; however, those that increase the APD are perhaps most common. Sodium channels are a key contributor to action potential generation and propagation (Catterall et al., 2005); therefore, disrupting these channels' ability to fast-inactivate could result in the elongation of the APD, which could prolong the QT interval leading to arrhythmogenicity. According to

TABLE 6 | Action potential duration.

	Time (ms)	Voltage (mV)
Wild-type		
$Na_V1.5$		
Control	198.3	−70.0
AMD 0.5 μM	204.4	−70.0
AMD 2.5 μM	224.3	−70.0
DES 0.5 μM	221.4	−70.0
DES 2.5 μM	231.9	−70.0
ΔKPQ		
$Na_V1.5$		
Control	230.4	−70.0
AMD 0.5 μM	235.2	−70.0
AMD 2.5 μM	230.2	−70.0
DES 0.5 μM	247.8	−70.0
DES 2.5 μM	496.1	−70.0

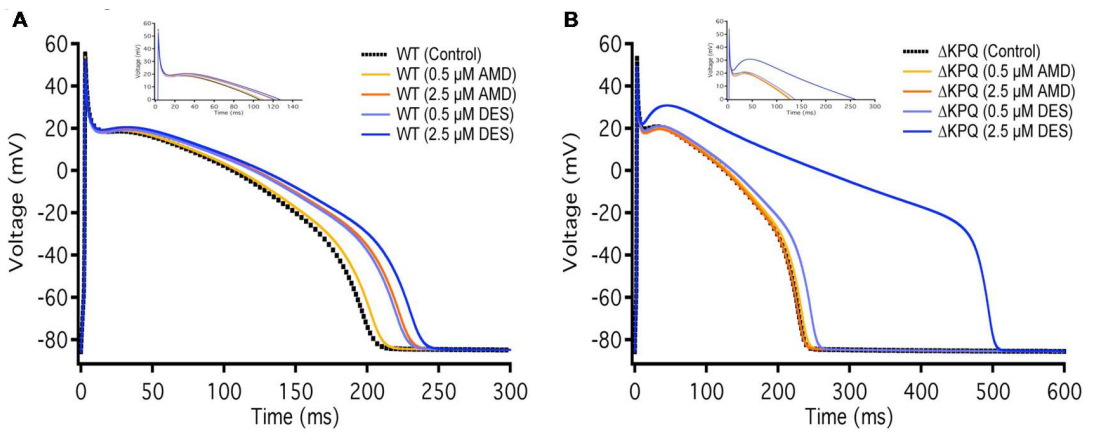

FIGURE 8 | Action potential model simulation. (A) Shows the simulations belonging to WT $Na_v1.5$, where the black curve represents control, light and dark orange curves represent AMD perfusion at 0.5 and 2.5 μM, respectively, and light and dark blue curves represent DES perfusion at 0.5 and 2.5 μM, respectively. **(B)** Shows the simulations belonging to ΔKPQ, where the black curve represents control, light and dark orange curves represent AMD perfusion at 0.5 and 2.5 μM, respectively, and light and dark blue curves represent DES perfusion at 0.5 and 2.5 μM, respectively.

our simulation results, AMD and DES indeed increase APD in myocytes. Thus, we conclude that these compounds could contribute to pro- arrhythmogenicity.

Despite the possibility of having pro-arrhythmic effects, our findings suggest that AMD and DES can also have an anti-arrhythmic effect in that they block $I_{Na,P}$. This mode of action is not unique to these compounds. Similar to AMD and DES, Wang et al. (1990) have shown that a compound called DPI 201-106 slows cardiac sodium channel inactivation, followed by blocking peak inward sodium currents.

N-desethylamiodarone seems to be a more potent pro-arrhythmic agent than the AMD from which it is metabolized. Since the LQT diagnosis is identified with an abnormally long QT interval, the use of AMD in a patient with this condition may be lethal. Therefore, our findings are a further validation for caution in the use of AMD in LQT patients, and specifically in those with the ΔKPQ mutation. Moreover, although AMD and DES have similar chemical structures, as we have shown, their effects on ionic sodium currents are not identical. Thus, we predict further characterization of AMD's long list of metabolites may uncover substantial clinically relevant information.

AUTHOR CONTRIBUTIONS

M-RG and MA collected, assembled, analyzed, and interpreted the data. PCR conceived the experiments and revised the manuscript critically for important intellectual content.

FUNDING

This work was supported by a grant from Natural Science and Engineering Research Council of Canada and the Canadian Foundation for Innovation.

ACKNOWLEDGMENTS

Thanks to Dr. Robert Kass for providing us with the ΔKPQ cDNA, and to Dr. Nabyl Merbouh for helping in AMD and DES attainment. Thanks to Dr. Ian Bercovitz for performing statistical analysis. Special thanks to Colin Peters for help in the interpretation of the results.

REFERENCES

Antzelevitch, C., and Burashnikov, A. (2009). Atrial-selective sodium channel block as a novel strategy for the management of atrial fibrillation. *J. Electrocardiol.* 42, 543–548. doi: 10.1016/j.jelectrocard.2009.07.007

Burashnikov, A., and Antzelevitch, C. (2013). Role of late sodium channel current block in the management of atrial fibrillation. *Cardiovasc. Drugs Ther.* 27, 79–89. doi: 10.1007/s10557-012-6421-1

Catterall, W. A., Goldin, A. L., and Waxman, S. G. (2005). International union of pharmacology. XLVII. nomenclature and structure-function relationships of voltage-gated sodium channels. *Pharmacol. Rev.* 57, 397–409. doi: 10.1124/pr.57.4.5

Chandra, R., Starmer, C. F., and Grant, A. O. (1998). Multiple effects of KPQ deletion mutation on gating of human cardiac na+ channels expressed in mammalian cells. *Am. J. Physiol.* 274(5 Pt 2), H1643–H1654.

Danzi, S., and Klein, I. (2015). Amiodarone-induced thyroid dysfunction. *J. Intensive Care Med.* 30, 179–185. doi: 10.1177/0885066613503278

Deng, P., You, T., Chen, X., Yuan, T., Huang, H., and Zhong, D. (2011). Identification of amiodarone metabolites in human bile by ultraperformance liquid chromatography/quadrupole time-of-flight mass spectrometry. *Drug Metab. Dispos.* 39, 1058–1069. doi: 10.1124/dmd.110.037671

Digby, G. C., Perez Riera, A. R., Barbosa Barros, R., Simpson, C. S., Redfearn, D. P., Methot, M., et al. (2011). Acquired long QT interval: a case series of multifactorial QT prolongation. *Clin. Cardiol.* 34, 577–582. doi: 10.1002/clc.20945

Franz, M. R., Gray, R. A., Karasik, P., Moore, H. J., and Singh, S. N. (2014). Drug-induced post-repolarization refractoriness as an antiarrhythmic principle and its underlying mechanism. *Europace* 16(Suppl. 4), iv39–iv45. doi: 10.1093/europace/euu274

Hund, T. J., and Rudy, Y. (2004). Rate dependence and regulation of action potential and calcium transient in a canine cardiac ventricular cell model. *Circulation* 110, 3168–3174. doi: 10.1161/01.CIR.0000147231.69595.D3

Kodama, I., Kamiya, K., and Toyama, J. (1997). Cellular electropharmacology of amiodarone. *Cardiovasc. Res.* 35, 13–29. doi: 10.1016/S0008-6363(97)00114-4

Le Bouter, S., El Harchi, A., Marionneau, C., Bellocq, C., Chambellan, A., van Veen, T., et al. (2004). Long-term amiodarone administration remodels expression of ion channel transcripts in the mouse heart. *Circulation* 110, 3028–3035. doi: 10.1161/01.CIR.0000147187.78162.AC

Lloyd, C. M., Lawson, J. L., Hunter, P. J., and Nielsen, P. F. (2008). The CellML model repository. *Bioinformatics* 24, 2122–2123. doi: 10.1093/bioinformatics/btn390

Maltsev, V. A., Sabbah, H. N., and Undrovinas, A. I. (2001). Late sodium current is a novel target for amiodarone: studies in failing human myocardium. *J. Mol. Cell. Cardiol.* 33, 923–932. doi: 10.1006/jmcc.2001.1355

Nattel, S., and Singh, B. N. (1999). Evolution, mechanisms, and classification of antiarrhythmic drugs: focus on class III actions. *Am. J. Cardiol.* 84, 11R–19R. doi: 10.1016/S0002-9149(99)00697-9

Ohyama, K., Nakajima, M., Nakamura, S., Shimada, N., Yamazaki, H., and Yokoi, T. (2000). A significant role of human cytochrome P450 2C8 in amiodarone N-deethylation: an approach to predict the contribution with relative activity factor. *Drug Metab. Dispos.* 28, 1303–1310.

Pallandi, R. T., and Campbell, T. J. (1987). Resting, and rate-dependent depression of vmax of guinea-pig ventricular action potentials by amiodarone and desethylamiodarone. *Br. J. Pharmacol.* 92, 97–103. doi: 10.1111/j.1476-5381.1987.tb11300.x

Phillips, B. G., and Bauman, J. L. (1995). Prescribing trends and pharmacoeconomic considerations in the treatment of arrhythmias. focus on atrial fibrillation and flutter. *Pharmacoeconomics* 7, 521–533. doi: 10.2165/00019053-199507060-00006

Pollak, P. T. (1998). Oral amiodarone: historical overview and development. *Pharmacotherapy* 18(6 Pt 2), 121S–126S.

Rogers, J. C., Qu, Y., Tanada, T. N., Scheuer, T., and Catterall, W. A. (1996). Molecular determinants of high affinity binding of alpha-scorpion toxin and sea anemone toxin in the S3-S4 extracellular loop in domain IV of the na+ channel alpha subunit. *J. Biol. Chem.* 271, 15950–15962. doi: 10.1074/jbc.271.27.15950

Sheldon, R. S., Hill, R. J., Cannon, N. J., and Duff, H. J. (1989). Amiodarone: biochemical evidence for binding to a receptor for class I drugs associated with the rat cardiac sodium channel. *Circ. Res.* 65, 477–482. doi: 10.1161/01.RES.65.2.477

Singh, B. N., and Vaughan Williams, E. M. (1970). The effect of amiodarone, a new anti-anginal drug, on cardiac muscle. *Br. J. Pharmacol.* 39, 657–667. doi: 10.1111/j.1476-5381.1970.tb09891.x

Suzuki, T., Morishima, M., Kato, S., Ueda, N., Honjo, H., and Kamiya, K. (2013). Atrial selectivity in Na+channel blockade by acute amiodarone. *Cardiovasc. Res.* 98, 136–144. doi: 10.1093/cvr/cvt007

Tarapues, M., Cereza, G., Arellano, A. L., Montane, E., and Figueras, A. (2014). Serious QT interval prolongation with ranolazine and amiodarone. *Int. J. Cardiol.* 172, e60–e61. doi: 10.1016/j.ijcard.2013.12.061

Wang, G., Dugas, M., Ben Armah, I., and Honerjager, P. (1990). Interaction between DPI 201-106 enantiomers at the cardiac sodium channel. *Mol. Pharmacol.* 37, 17–24.

Wang, Q., Shen, J., Splawski, I., Atkinson, D., Li, Z., Robinson, J. L., et al. (1995). SCN5A mutations associated with an inherited cardiac arrhythmia, long QT syndrome. *Cell* 80, 805–811. doi: 10.1016/0092-8674(95)90359-3

Wu, L., Rajamani, S., Shryock, J. C., Li, H., Ruskin, J., Antzelevitch, C., et al. (2008). Augmentation of late sodium current unmasks the proarrhythmic effects of amiodarone. *Cardiovasc. Res.* 77, 481–488. doi: 10.1093/cvr/cvm069

Zahno, A., Brecht, K., Morand, R., Maseneni, S., Torok, M., Lindinger, P. W., et al. (2011). The role of CYP3A4 in amiodarone-associated toxicity on HepG2 cells. *Biochem. Pharmacol.* 81, 432–441. doi: 10.1016/j.bcp.2010.11.002

Zipes, D. P., Prystowsky, E. N., and Heger, J. J. (1984). Amiodarone: electrophysiologic actions, pharmacokinetics and clinical effects. *J. Am. Coll. Cardiol.* 3, 1059–1071. doi: 10.1016/S0735-1097(84)80367-8

Conflict of Interest Statement: The authors declare that the research was conducted in the absence of any commercial or financial relationships that could be construed as a potential conflict of interest.